Journal of
Applied Crystallography

ISSN 0021-8898

Received 18 September 2006
Accepted 20 December 2006

On the entropy to texture index relationship in quantitative texture analysis

R. Hielscher,[a] H. Schaeben[a]* and D. Chateigner[b]

[a]Technische Universität Bergakademie Freiberg, Institut für Geologie, B. v. Cotta Str. 2, 09599 Freiberg, Germany, and [b]CRISMAT–ENSICAEN, Université de Caen Basse–Normandie, 6 Bd. M. Juin, 14050 Caen, France. Correspondence e-mail: schaeben@geo.tu-freiberg.de

This communication demonstrates a sharp inequality between the L^2-norm and the entropy of probability density functions. This inequality is applied to texture analysis, and the relationship between the entropy and the texture index of an orientation density function is characterized. More precisely, the orientation space is shown to allow for texture index and entropy variations of orientation probability density functions between an upper and a lower bound for the entropy. In this way, it is proved that there is no functional relationship between entropy and texture index of an orientation probability density function as conjectured previously on the basis of practical numerical texture analyses using the widely used pole-to-orientation probability density function reconstruction software *WIMV*, known by the initials of its authors and their ancestors (Williams–Imhof–Matthies–Vinel). Synthetic orientation probability density functions were then synthesized, covering a large domain of variation for texture index and entropy, and used to check the numerical results of the same software package.

1. Introduction

In quantitative texture analysis (QTA), the most frequently used measure to quantify the texture strength, *i.e.* the extent of preferred orientation, on which most of the macroscopic properties of anisotropic materials depend, is the texture index, F (Bunge, 1982). The texture index aids in comparing the overall texture evolution of sample series, provided texture components of the same type are present in the polycrystalline aggregate. Another measure of the overall texture strength is the entropy S, which actually measures the deviation from the uniform texture or lack of 'organization' of orientations (Schaeben, 1988). Both quantities F and S are calculated from the orientation probability density function (ODF) of the crystallites. In the texture community it has recently been assumed that both the entropy and the texture index can be used to detect possible discrepancies or artefacts introduced by the numerical ODF reconstruction from experimental diffraction data (Chateigner, 2005). However, the exact relationship of the two quantities was theoretically not well understood, nor were the mathematical assumptions and practical prerequisites of the ODF reconstruction software *WIMV* (Matthies & Vinel, 1982), designed to recover and explain experimental data, sufficiently carefully examined.

In this short communication, after the general definition of the entropy and the texture index as the L^2-norm of a probability density function, we initially consider the class of probability density functions taking only two different values. For this class of probability density functions, we prove that the entropy is bounded by zero and the negative logarithm of the L^2-norm. Then we show that the class was chosen to be sufficiently large to characterize the relationship between the entropy and the L^2-norm of probability density functions completely. Correspondingly, the next theoretical section is basically organized as a sequence of mathematical definitions, propositions and short proofs.

In the section devoted to practical numerical texture analysis, we then examine how simulated ODFs with various texture index and entropy values are recovered using the widely used ODF reconstruction algorithm *WIMV* (Matthies & Vinel, 1982) as incorporated in *Beartex* (Wenk *et al.*, 1998). From this analysis, we illustrate the limitations of the actual software in terms of texture strengths for common experimental designs with a resolution of the order of 5°.

2. Theory

We start with a formal definition of the entropy and the L^2-norm of a probability density function.

Let (X, μ) be a probability space and let $f: X \to \mathbb{R}$ be a square integrable probability density function. The entropy S and the L^2-norm $\|\cdot\|_2$ of f are defined by

$$S = -\int_X f(x) \ln f(x)\, \mathrm{d}\mu(x) \quad \text{and} \quad F = \|f\|_2^2 = \int_X f(x)^2\, \mathrm{d}\mu(x).$$

Let X be the orientation space SO(3) (*cf.* Morawiec, 2004). Then there is a rotationally invariant probability measure μ, called the Haar measure, of the compact group SO(3). The ODF can be seen as a probability density function defined on the probability space $(\mathrm{SO3}, \mu)$. In this context the L^2-norm of a square integrable ODF is called its texture index.

First of all we note that because $|f(x)\ln f(x)| \leq f(x)^2$ for $f(x) \geq 1$ and $|f(x)\ln f(x)| \leq 1$ for $f(x) \in [0, 1]$ the entropy is well defined for the class of all square integrable probability density functions. Furthermore, we notice that the relationship between the entropy and the texture index might be completely investigated considering monotonically increasing functions on $X = [0, 1]$ only. More precisely, we have the following first proposition.

Proposition 1: Let f be a square integrable probability density function on an arbitrary probability space (X, μ). Then there is a square integrable, monotonically increasing probability density function $\tilde{f} : ([0, 1], \lambda) \to \mathbb{R}$ such that $S(f) = S(\tilde{f})$ and $\|f\|_2 = \|\tilde{f}\|_2$. Here λ denotes the Borel–Lebesgue measure (Halmos, 1950).

The proof is given as follows. Let $f : X \to \mathbb{R}$ be a simple function, *i.e.* a function taking only a finite number of values $f_1 \leq f_2 \leq \ldots \leq f_N$. Then we define a monotonically increasing function $\tilde{f}$ on $[0, 1]$ by setting $\tilde{f}(x) = f_i$ for

$$x \in \Big(\sum_{j=1}^{i-1} \mu[f^{-1}(f_j)], \sum_{j=1}^{i} \mu[f^{-1}(f_j)]\Big].$$

In particular, $\tilde{f}$ possesses the properties $\int_0^1 \tilde{f}(x)\,\mathrm{d}x = 1$, $S(f) = S(\tilde{f})$ and $\|f\|_2 = \|\tilde{f}\|_2$. Using approximation by simple functions these properties are generalized to the class of square integrable functions.

Next we exemplify our first proposition, which allows us to focus our attention on the class of square integrable, monotonically increasing probability density functions on $[0, 1]$.

Let $x_1 \in [0, 1]$ and $0 \leq y_1 \leq y_2$. We define a monotonically increasing probability density function f_{x_1,y_1} that takes only the two values y_1 and y_2

$$f_{x_1,y_1}(x) = \begin{cases} y_1 & 0 \leq x \leq x_1, \\ y_2 & x_1 < x \leq 1. \end{cases}$$

Setting $y_2 = (1 - x_1y_1)/(1 - x_1)$, we ensure $\int_0^1 f_{x_1,y_1}(x)\,\mathrm{d}x = 1$, the usual normalization of any probability density function. Now the entropy and the L^2-norm of f_{x_1,y_1} can be explicitly given in terms of x_1 and y_1:

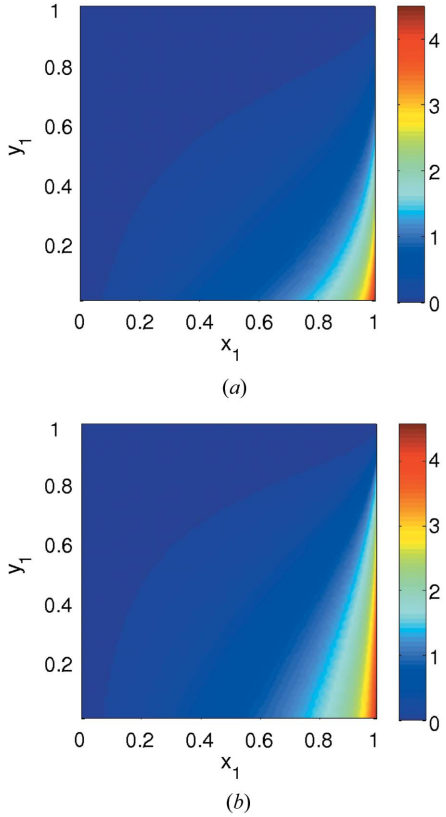

Figure 1
(*a*) Negative entropy $-S$ and (*b*) logarithm of the L^2-norm $\log(F)$ of f_{x_1,y_1} for $x_1, y_1 \in [0, 1]$.

$$\begin{aligned} S(x_1, y_1) &= -x_1y_1 \ln y_1 - (1 - x_1)y_2 \ln y_2 \\ &= -x_1y_1 \ln y_1 - (1 - x_1y_1) \ln \frac{1 - x_1y_1}{1 - x_1}, \\ F(x_1, y_1) &= x_1y_1^2 + (1 - x_1)y_2^2 = \frac{1 - 2x_1y_1 + x_1y_1^2}{1 - x_1}. \end{aligned}$$

Fig. 1 completes the example and shows the negative entropy and the logarithm of the L^2-norm of the function f_{x_1,y_1} plotted as function of x_1 and y_1. Both plots look very similar, only deviating from each other for large values of x_1.

Let us fix the L^2-norm $\tilde{F} \geq 1$. Then f_{x_1,y_1} has the L^2-norm $\tilde{F}$ if and only if $x_1 \in [(\tilde{F} - 1)/\tilde{F}, 1)$ and $y_1 = \tilde{y}_1(x_1) = 1 - \{[(1 - x_1)/x_1] \times (\tilde{F} - 1)\}^{1/2}$. Hence, for every $x_1 \in [(\tilde{F} - 1)/\tilde{F}, 1)$ there is an unique probability density function $\tilde{f}_{x_1} = f_{x_1,\tilde{y}_1(x_1)} = f_{x_1,1-\{[(1-x_1)/x_1](\tilde{F}-1)\}^{1/2}}$ that has L^2-norm $\tilde{F}$. Simple calculations show that $\tilde{y}_1(x_1)$ is monotonically increasing for $x_1 \in [(\tilde{F} - 1)/\tilde{F}, 1)$ and $\tilde{y}_2(x_1) = [1 - x_1\tilde{y}_1(x_1)]/(1 - x_1)$ is monotonically decreasing. In Fig. 2 the paths $y_1 = \tilde{y}_1(x_1)$, or iso-F lines, are plotted for different values of $\tilde{F} = 1.01$, 1.2, 2, 5, 20. The second proposition states that the entropy of $\tilde{f}_{x_1}$ increases monotonically along these paths.

Proposition 2: Let $\tilde{F} \geq 1$ and $\tilde{f}_{x_1} = f_{x_1,\tilde{y}_1(x_1)}$ as described above. Denote $\tilde{S}(x_1) = S[x_1, \tilde{y}_1(x_1)]$ the entropy of $\tilde{f}_{x_1}$. Then $\tilde{S}(x_1)$ is a continuous, monotonically increasing function on $[(\tilde{F} - 1)/\tilde{F}, 1)$ with $\tilde{S}[(\tilde{F} - 1)/\tilde{F}] = -\ln \tilde{F}$ and $\lim_{x_1 \to 1} \tilde{S}(x_1) = 0$.

We give the following proof. Since $\tilde{y}_1(x_1) = 1 - \{[(1 - x_1)/x_1] \times (\tilde{F} - 1)\}^{1/2}$ is continuous on $[(\tilde{F} - 1)/\tilde{F}, 1)$ the entropy $\tilde{S}(x_1)$ is also continuous. For the boundary point $x_1 = (\tilde{F} - 1)/\tilde{F}$, we obtain $\tilde{y}_1(x_1) = 0$ and hence,

$$\tilde{S}\left(\frac{\tilde{F} - 1}{\tilde{F}}\right) = -\ln F_0.$$

Elementary calculations show that for $x_1 \to 1$, we have $\lim_{x_1 \to 1} \tilde{S}(x_1) = 0$.

In order to prove monotonicity, we show $\mathrm{d}\tilde{S}(x_1)/\mathrm{d}x_1 \geq 0$. The partial derivatives of $S(x_1, y_1)$ and $F(x_1, y_1)$ are calculated to

$$\begin{aligned} \partial_1 S(x_1, y_1) &= -\frac{1 - y_1}{1 - x_1} + y_1 \ln \frac{1 - x_1y_1}{(1 - x_1)y_1}, \\ \partial_2 S(x_1, y_1) &= x_1 \ln \frac{1 - x_1y_1}{(1 - x_1)y_1}, \\ \partial_1 F(x_1, y_1) &= \left(\frac{1 - y_1}{1 - x_1}\right)^2, \\ \partial_2 F(x_1, y_1) &= -\frac{2x_1(1 - y_1)}{1 - x_1}. \end{aligned}$$

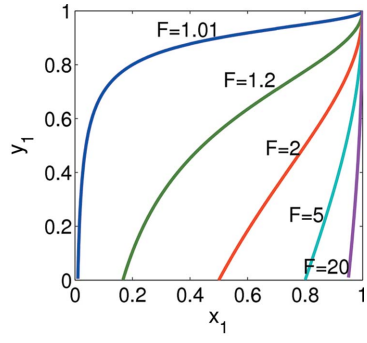

Figure 2
The paths $\tilde{y}_1(x_1)$ of constant L^2-norm F.

The derivative $\mathrm{d}\tilde{S}/\mathrm{d}x_1 = \mathrm{d}S[x_1, \tilde{y}_1(x_1)]/\mathrm{d}x_1$ is the directional derivative of S along the contour line of $F(x_1, y_1) = \tilde{F}$. Since the gradient of F is orthogonal to the contour line, we obtain

$$\begin{aligned}\frac{\mathrm{d}}{\mathrm{d}x_1}\tilde{S}(x_1) &= \nabla S[x_1, \tilde{y}_1(x_1)]\Big\{\partial_2 F[x_1, \tilde{y}_1(x_1)], -\partial_1 F[x_1, \tilde{y}_1(x_1)]\Big\} \\ &= \partial_1 S[x_1, \tilde{y}_1(x_1)]\,\partial_2 F[x_1, \tilde{y}_1(x_1)] \\ &\quad - \partial_2 S[x_1, \tilde{y}_1(x_1)]\,\partial_1 F[x_1, \tilde{y}_1(x_1)] \\ &= \frac{x_1(1-\tilde{y}_1)}{(1-x_1)^2}\left[2(1-\tilde{y}_1) - (1+\tilde{y}_1 - 2x_1\tilde{y}_1)\ln\frac{(1-x_1)\tilde{y}_1}{1-x_1\tilde{y}_1}\right].\end{aligned}$$

Since for all $x_1, y_1 \in (0, 1)$ we have $x_1(1-y_1)/(1-x_1)^2 \geq 0$ and

$$\frac{2(1-y_1)}{1+y_1-2x_1y_1} \geq 0 \geq \ln\frac{(1-x_1)y_1}{1-x_1y_1},$$

we conclude that $\mathrm{d}\tilde{S}(x_1)/\mathrm{d}x_1 \geq 0$, which completes the proof.

We note that our second proposition immediately implies that there is no functional relationship of entropy and L^2-norm but that the entropy may vary substantially for a given L^2-norm. Since for a fixed L^2-norm $\tilde{F}$ of $f_{x_1,\tilde{y}_1(x_1)}$ the minimum value $\tilde{y}_1(x_1)$ of $f_{x_1,\tilde{y}_1(x_1)}$ is a strictly monotonically increasing function of x_1, there is a strictly monotonically increasing function $\tilde{x}_1 : [0, 1) \rightarrow \mathbb{R}$ such that $f_{\tilde{x}_1(y_1),y_1}$ has texture index $\tilde{F}$ for all $y_1 \in [0, 1)$. Now our second proposition implies that the entropy $S[x_1, \tilde{y}_1(x_1)]$ of $f_{\tilde{x}_1(y_1),y_1}$ is a monotonically increasing function of $y_1 \in [0, 1)$. In particular we have for $x_1 = \tilde{x}_1(y_1)$

$$S(x_1, y_1) = -\frac{(\tilde{F}-1)y_1}{\tilde{F}-1+(1-y_1)^2}\ln y_1 - \frac{(\tilde{F}-y_1)(1-y_1)}{\tilde{F}-1+(1-y_1)^2}\ln\frac{\tilde{F}-b}{1-b}. \tag{1}$$

Up to now our demonstration concerned probability density functions taking only two values. However, even under such restriction, we found that probability density functions corresponding to any (S, F) pair exist, with the lower bound of $S \geq -\ln F$.

With our third proposition, we show that there are no square integrable probability density functions corresponding to pairs (S, F) with $S < -\ln F$.

Proposition 3: Let f be a monotonically increasing probability density function on $[0, 1]$ taking only the three different values, y_1, y_2 and y_3, with $0 \leq y_1 \leq y_2 \leq y_3$ and $0 \leq x_1 \leq x_2$, such that

$$f(x) = \begin{cases} y_1 & 0 \leq x < x_1, \\ y_2 & x_1 \leq x < x_2, \\ y_3 & x_2 \leq x \leq 1. \end{cases}$$

Then there are monotonically increasing probability density functions f_- and f_+ with $\min_{x\in[0,1]} f_-(x) \geq \min_{x\in[0,1]} f(x)$ and $\min_{x\in[0,1]} f_+(x) \geq \min_{x\in[0,1]} f(x)$ that take only two values, y_1, y_2 and y_2, y_3, respectively, and satisfy $\|f\|_1 = \|f_-\|_1 = \|f_+\|_1$, $\|f\|_2 = \|f_-\|_2 = \|f_+\|_2$ and $S(f_-) \leq S(f) \leq S(f_+)$. Our proof is an application of our first proposition. Restricting f to $[x_1, 1]$, we can apply the two-valued case. In particular, there are monotonic, continuous functions $\tilde{y}_2 : [x_1, 1] \rightarrow \mathbb{R}_+$ and $\tilde{y}_3 : [x_1, 1] \rightarrow \mathbb{R}_+$ with $y_1 \leq \tilde{y}_2 \leq \tilde{y}_3$ such that for all $\tilde{x}_2 \in [x_1, 1)$ the function

$$f_{\tilde{x}_2}(x) = \begin{cases} y_1 & 0 \leq x < x_1, \\ \tilde{y}_2(\tilde{x}_2) & x_1 \leq x < \tilde{x}_2, \\ \tilde{y}_3(\tilde{x}_2) & \tilde{x}_2 \leq x \leq 1, \end{cases}$$

preserves the L^1-norm and L^2-norm, respectively. Moreover, by our second proposition, we know that the entropy $S(\tilde{x}_2)$ of $f_{\tilde{x}_2}$ decreases monotonically when $\tilde{x}_2$ decreases. In the case that $y_1 = \tilde{y}_2(\tilde{x}_2)$ the function $f_- = f_{\tilde{x}_2}$ is a two-valued function that preserves the ^{1}-norm and the L^2-norm, respectively, and has smaller entropy than f.

Focusing on the restriction of f to $[0, x_2]$, we analogously obtain a function f_+ that preserves the L^1- and L^2-norm, respectively, and has larger entropy than f. Thus, our proof is completed.

We are now able to formulate our major result characterizing the relationship between the entropy and the L^2-norm of a probability density function.

Proposition 4: Let f be a square integrable probability density function and denote $f_{\min} = \min_{x\in[0,1]} f(x)$ its minimum value. Then we have the following relationship between the L^2-norm F and entropy S of f:

$$S \geq -\frac{(F-1)f_{\min}}{F-1+(1-f_{\min})^2}\ln f_{\min} - \frac{(F-f_{\min})(1-f_{\min})}{F-1+(1-f_{\min})^2}\ln\frac{F-f_{\min}}{1-f_{\min}}. \tag{2}$$

In particular we have

$$0 \geq S \geq -\ln F. \tag{3}$$

Conversely, for every pair $F \geq 1$ and $0 > S \geq -\ln F$ of L^2-norm and entropy there is a corresponding probability density function f. Actually, our second proposition and its explicit implication prove the theorem for any function f defined by only two values. Applying the third proposition, induction yields the proof of inequality equations (2) and (3) for all simple functions. The general case is obtained by approximation of any square integrable probability density function with simple functions. It should be noted that a pair $F \geq 1$ and $0 > S \geq -\ln F$ of L^2-norm and entropy does not uniquely determine a probability density function f.

Although Fig. 1 suggests a very close relationship between the entropy and the L^2-norm of a square integrable probability density function f, we have shown in our fourth proposition that for a fixed L^2-norm the entropy of f may vary between zero and the negative logarithm of the L^2-norm of f. As a rule of thumb, we conclude that the entropy is close to zero if the minimum value $f_{\min}$ is close to one and conversely that the entropy is close to the negative logarithm of the L^2-norm of f if f has large regions close to zero.

The region of all admissible combinations of the L^2-norm and the entropy of square integrable probability density functions interpreted as the ODF space is illustrated in Fig. 3. In this figure one clearly sees the lower bound for the entropy respecting equation (2) for different minimum values of the ODF f, *i.e.* for $f_{\min} \in \{\frac{2}{3}, \frac{1}{3}, 0\}$. The lower bound $-\ln F$ for the general case $f_{\min} \geq 0$ is the smallest lower bound. The most interesting point here contrary to previous observations (Chateigner, 2005) is that for values of the entropy S close to 0 any texture index value can exist, and that for a given value of the texture index F the entropy S may vary between 0 and $-\ln F$. Since

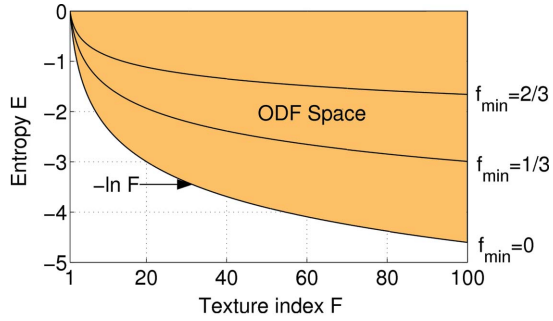

Figure 3
The ODF space as seen from texture index and entropy.

our mathematical development is general and valid for any ODF it remains to understand why almost always $S \simeq -\ln F$ was observed for real and simulated data by Chateigner (2005).

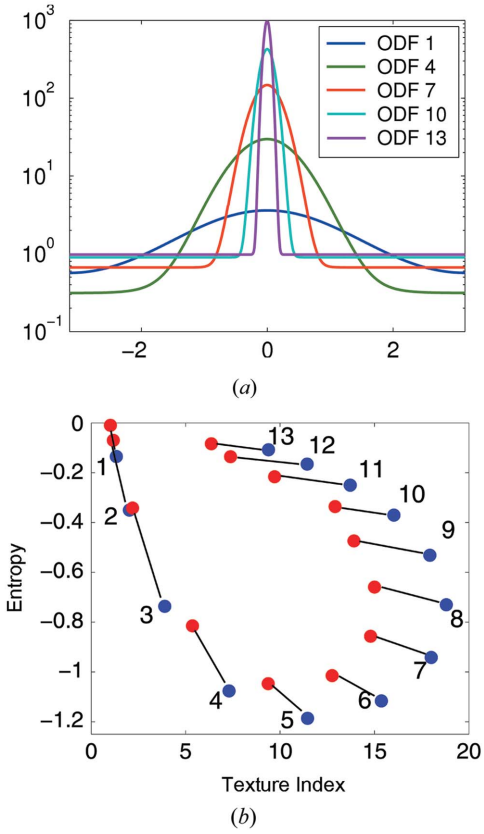

Figure 4
(*a*) Some of the synthetic ODFs and (*b*) their texture index–entropy relationship depicted as blue dots. The red dots represent the texture index–entropy relationship of the *WIMV*-reconstructed ODFs. The numbers refer to the enumeration of the synthetic ODFs starting in the upper-left corner and counting anticlockwise.

3. ODF reconstruction with simulated data

In order to clarify this last point, we generated a total of 13 synthetic ODFs with values for texture index F and the entropy S as plotted in Fig. 4. All these ODFs were constructed for triclinic crystal symmetry with $a = b = c$ and $\alpha = \beta = \gamma = 90^\circ$ as the superposition of a uniformly distributed component and a von Mizes–Fisher distributed component centered at $g_0 = \{0, 0, 0\}$. From these ODFs, we calculated the {001}, {010}, {100}, {111}, $\{\bar{1}11\}$, $\{1\bar{1}1\}$ and $\{\bar{1}\bar{1}1\}$ pole figures on a $5 \times 5^\circ$ grid. Applying the *WIMV* algorithm with minimum convergence rate 0.1 to the pole figure data, we computed approximations of the 13 synthetic ODFs. The results of the reconstruction and a comparison with the original ODFs are given in Table 1. We observe that the given pole figures are sufficiently well approximated by the recalculated pole figures (RP0 $\leq 0.5\%$), whereas the entropy and the texture index of the recalculated ODFs are far away from the initial values (see Fig. 4). One recognizes that the RP1 error becomes larger for the ODFs with a sharper preferred component. This is due to our restriction to a $5 \times 5^\circ$ grid.

The texture index *versus* entropy plot 4 of the synthetic and reconstructed ODFs clearly shows that they are not located on the lower bound $-\ln F = S$, which is an empirical evidence that this lower bound can generally not be used as a criterion to check the goodness of fit of numerically reconstructed ODFs, as was suggested by Chateigner (2005). Interestingly enough, texturation processes are often developing texture components at the expense of the uniform portion, thus rapidly stabilizing textures without a uniform portion. In this case we can expect texture index–entropy combinations that are located close to the lower bound.

Chateigner (2005) analyzed only strongly textured samples. The corresponding ODFs plotted by Chateigner (2005, Figs. 5*b* and 6*a* therein) do not contain uniform components, except for few samples with small texture index F for which reconstruction discrepancies overlap the presence of the uniform component. Fig. 5 verifies that for these ODFs the pairs (F, S) are located close to the lower bound $S = -\ln F$.

As a global trend, samples with ODFs having arbitrary texture index F and entropy S with $-\ln F \leq S \leq 0$ exist. ODFs with a weakly preferred smooth texture component and large uniform portion will

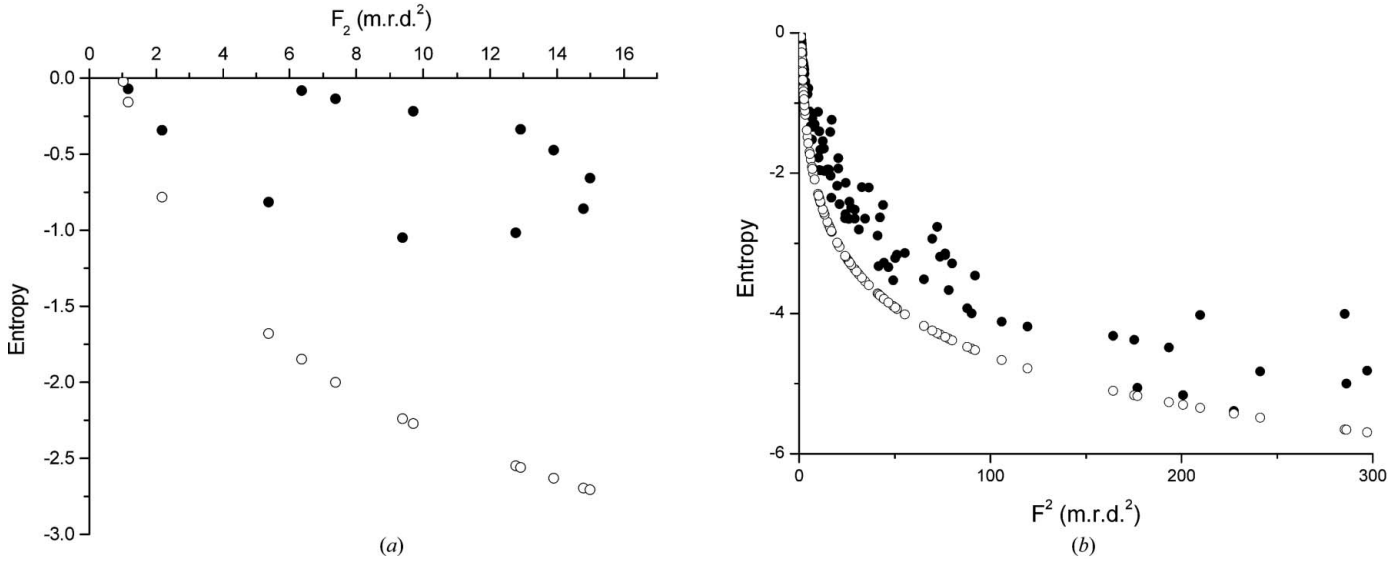

Figure 5
F–*S* plot of the simulated ODFs (full circles) and of the lower bound (open circles) for (*a*) the simulated ODFs of this work and (*b*) the experimental ODFs of Chateigner (2005).

Table 1
Simulated ODFs and ODFs reconstructed with the *WIMV* algorithm of *Beartex*, and reconstruction parameters.

	Simulated ODF				Recalculated ODF				Error	
ID	Min. (m.r.d.)	Max.	F (m.r.d.^{2})	S	Min. (m.r.d.)	Max.	F (m.r.d.^{2})	S	RP0 (%)	RP1 (%)
1	0.57	3.6	1.33	−0.135	0.81	1.87	1.02	−0.009	0.30	0.31
2	0.14	6.8	2.02	−0.350	0.57	4.19	1.17	−0.070	0.32	0.29
3	0.21	14.6	3.89	−0.736	0.24	11.20	2.19	−0.342	0.46	0.26
4	0.31	29.8	7.30	−1.076	0.10	26.52	5.36	−0.815	0.49	0.22
5	0.42	55.1	11.45	−1.186	0.13	51.72	9.37	−1.047	0.42	0.40
6	0.55	93.5	15.36	−1.116	0.23	88.43	12.76	−1.014	0.58	0.53
7	0.67	147.7	18.00	−0.941	0.29	136.26	14.79	−0.856	0.62	0.71
8	0.77	219.8	18.80	−0.730	0.35	195.38	15.00	−0.659	0.63	0.96
9	0.85	311.7	17.93	−0.531	0.37	268.74	13.91	−0.473	0.54	0.96
10	0.90	427.0	16.02	−0.370	0.30	381.86	12.91	−0.336	0.53	1.06
11	0.94	571.3	13.71	−0.250	0.34	471.96	9.71	−0.216	0.73	3.80
12	0.96	752.3	11.43	−0.165	0.43	638.02	7.38	−0.136	0.87	6.64
13	0.98	980.7	9.39	−0.107	0.44	799.64	6.36	−0.084	0.71	8.16

be located close to small F and large S, while ODFs with large areas close to zero will be located close to the lower bound $-\ln F$. Finally, ODFs with a large uniform portion but very sharp texture components will have entropy S close to zero but a large texture index F. Such samples will necessarily exhibit textured components with very narrow half-width, which will require largely improved measurement resolution, *i.e.* scanning grids with refined meshes, and appropriate software which is adapted for their reconstruction. This is why we observe a larger deviation of reconstructed data from the lower bound (Fig. 5) for large texture indices than for small texture indices.

4. Conclusion

We have characterized the ODF space in terms of texture index and entropy. We have demonstrated that this space is not confined to the previously observed single continuous line $S = -\ln F$, but that this line actually corresponds to a lower bound corresponding to ODFs without a uniform component. In general ODFs can be located between this lower bound and the upper bound 0, where the only possible point on the upper bound is $(S, F) = (0, 1)$ for the uniform texture. Simulated and experimental data taken from a previous work confirm our findings.

References

Bunge, H. J. (1982). *Texture Analysis in Materials Science*. London: Butterworths.
Chateigner, D. (2005). *J. Appl. Cryst.* **38**, 603–611.
Halmos, P. (1950). *Measure Theory*. Princeton, NJ: Van Nostrand.
Matthies, S. & Vinel, G. W. (1982). *Phys. Status Solidi B*, **112**, K111.
Morawiec, A. (2004). *Orientations and Rotations, Computations in Crystallographic Textures*. Berlin: Springer.
Schaeben, H. (1988). *J. Appl. Phys.* **64**, 2236–2237.
Wenk, H.-R., Matthies, S., Donovan, J. & Chateigner, D. (1998). *J. Appl. Cryst.* **31**, 262.